

# Exercise Fatigue Monitoring Based on R-Peak Detection Using UNET-TCN

Xinhua Su, Xuxuan Wang<sup>✉</sup>, Xinxin Ma

**Abstract:** Moderate exercise contributes to health, but excessive exercise may lead to physical injury or even endanger life. It is pressing for a device that can detect the intensity of exercise. Therefore, in order to enable real-time detection of exercise intensity and mitigate the risks of harm from excessive exercise, a exercise intensity monitoring system based on the heart rate variability (HRV) from electrocardiogram (ECG) signal and linear features from phonocardiogram (PCG) signal is proposed. The main contributions include: First, accurate analysis of HRV is crucial for subsequent exercise intensity detection. To enhance HRV analysis, we propose an R-peak detector based on encoder-decoder and temporal convolutional network (TCN). Experimental results demonstrate that the proposed R-peak detector achieves an F1 score exceeding 0.99 on real high-intensity exercise ECG datasets. Second, an exercise fatigue monitoring system based on multi-signal feature fusion is proposed. Initially, utilizing the proposed R-peak detector for HRV extraction in exercise intensity detection, which outperforms traditional algorithms, with the system achieving a classification performance of 0.933 sensitivity, 0.802 specificity, and 0.960 accuracy. To further improve the system, we combine HRV with the linear features of PCG. Our exercise intensity detection system achieves 90.2% specificity, 96.7% recall, and 98.1% accuracy in five-fold cross-validation.

**Keywords:** heart rate variability (HRV); phonocardiogram (PCG); Unet; temporal convolutional network (TCN); machine learning; exercise intensity

## 1 Introduction

With the development of society, more and more people are engaging in daily exercise. However, inappropriate exercise intensity can lead to serious health problems [1], including sports injuries and even sudden death. Therefore, there is a pressing need for a device to monitor exercise intensity in real-time [2]. Exercise intensity detection not only helps exercisers better assess

their current physical condition [3–4], but also assists them in adjusting their exercise intensity, thereby truly achieving personalized training and optimizing exercise effects. In recent years, exercise intensity detection has attracted widespread attention in the fields of sports science and health monitoring. This technology aims to accurately access the level of exercise intensity [5–8]. Bok used the ventilation threshold to classify the exercise intensity [9]. Pero provided personalized exercise reports based on various biochemical parameters, including pH, white blood cells, red blood cells, proteins, and glucose [10]. However, these methods typically require specialized equipment and technical support, making them challenging to implement in daily exercise and unsuitable for real-time monitoring. Following the rapid advancement of deep learning, these

---

Manuscript received Feb. 27, 2024; revised Apr. 29, 2024; accepted May 15, 2024. The associate editor coordinating the review of this manuscript was Dr. Xudong Zhao. This work was supported in part by the National Natural Science Foundation of China (No. 62301056) and the Fundamental Research Funds for Central Universities (No. 2022QN005).

Xinhua Su, Xuxuan Wang and Xinxin Ma are with School of Sports Engineering, Beijing Sport University, Beijing 100091, China.

✉ Corresponding author. Email: [wxx0419@bsu.edu.cn](mailto:wxx0419@bsu.edu.cn)

DOI: [10.15918/j.jbit1004-0579.2024.026](https://doi.org/10.15918/j.jbit1004-0579.2024.026)

challenges were effectively addressed owing to its robust information extraction capabilities. Dong et al proposed a method for recognizing adolescent exercise intensity utilizing long short-term memory (LSTM) and ECG signals, yielding an impressive accuracy of 99.40% [11]. Similarly, Chen et al conducted classification of exercise fatigue utilizing image and linear features extracted from ECG data, achieving an accuracy of 94.32% [12]. Nonetheless, many of these models demand substantial computational resources, presenting obstacles for real-time exercise intensity detection.

In the ECG, HRV is a crucial indicator which measures the variation in time intervals between consecutive heartbeats and is effective in assessing overall health and fitness levels. During exercise, changes in HRV patterns reflect the body's response to physical exertion, making it a valuable indicator of exercise intensity [13]. As is well known, accurate detection of R-peaks is crucial in analyzing HRV. Therefore, a reliable R-peak detector is the key to the exercise intensity detection system. However, the traditional R-peak detector is developed for ECG measurements under static conditions. For instance, algorithms based on Pan and Tompkins enhance QRS features to detect R-peaks and then apply threshold filtering [14]. These algorithms lack robustness against noise and fail to adapt to changes in ECG during high-intensity exercise. With the advancement of deep learning, it has demonstrated excellent performance in R-peak detection. Laitala proposed R-peak detection using LSTM networks, which excelled at temporal modeling tasks involving long-term dependencies, thus making them suitable for ECG analysis [15]. Similarly, Zahid proposed a deep learning-based method using U-Net combined with Inception and Residual blocks. This approach achieved around 99.83% F1-score, 99.85% recall, and 99.82% precision on MIT-DB [16]. LSTM networks are considered more suitable for time series signals compared to other types of neural

networks, due to the ability to handle temporal modeling tasks by retaining long-term dependencies. Convolutional neural networks (CNNs) effectively enhance the speed of R-peak detection compared to recurrent neural networks (RNNs). Combining the advantages of both approaches, an R-peak detector based on Unet and TCN is proposed to achieve more precise R-peak position detection. Then, the HRV features of ECG signals are combined with the linear features of PCG signals, and the detection effect is further improved, which provides insight into the exercise intensity detection with multi-modal fusion.

To sum up, the contributions of this work are twofold:

- 1) An R-peak detector based on Unet-TCN is proposed, which combines the advantages of UNET and TCN. This integration effectively captures the spatial and temporal dependencies in ECG signals.
- 2) An exercise fatigue monitoring system based on multi-signal feature fusion is developed, which extracts additional features relevant for fatigue detection.
- 3) The proposed R-peak detector demonstrates significant superiority over traditional algorithms and exercise fatigue monitoring system based on multi-signal feature enhances the accuracy by 2.1% compared to solely relying on HRV from ECG signals.

The rest of the paper is organized as follows: Section 2 introduces the datasets used in our study; Section 3 presents the proposed method in detail; and Section 4 concludes and discusses on this work.

## 2 Datasets

### 2.1 GUDB Database

Data from the dataset related to physical activity is used for training the R-peak detector. The Dyspnea Database from the University of Glasgow (GUDB) [17] consists of ECG records from

25 subjects. The ECG signals were sampled at a frequency of 250 Hz.

## 2.2 EPFL Database

This dataset is utilized to evaluate the performance of the R-peak detection. The data is from the École Polytechnique Fédérale de Lausanne (EPFL) (<https://zenodo.org/records/5727800>) and is collected during high-intensity exercise. The ECG signals were initially sampled at a frequency of 500 Hz and subsequently down-sampled to 250 Hz. The ECG data segments contain various exercise stages, including preliminary and post ventilatory threshold, preliminary and mid maximum oxygen consumption (VO<sub>2</sub>max), and recovery.

## 2.3 EPHNOGRAM

The dataset is utilized to evaluate the exercise intensity detection system. The EPHNOGRAM dataset [18] records ECG and PCG data at a sampling rate of 8 kHz. These data are collected during various activities including resting, walk-

ing, running, cycling, etc. This dataset can be used for multi-modal attempts at exercise intensity detection.

## 3 Method

The study aims to develop an end-to-end exercise intensity detection system. Fig. 1 shows the development process. The first part is the R-peak detector. The cores are the model and wrapper function. In the second part, we embed the proposed R-peak detector in the system, which combines HRV from ECG with linear features from PCG to achieve exercise intensity detection.

### 3.1 R-Peak Detection

#### 3.1.1 Problem Formulation

The encoder-decoder comprises an encoder and a decoder. The encoder encodes the input signal into  $z(i)$ , and the decoder maps these features back to  $\hat{y}(i)$  using the following equations

$$\begin{aligned} z &= E(x; \theta) \\ \hat{y} &= D(z; \varphi) \end{aligned} \quad (1)$$

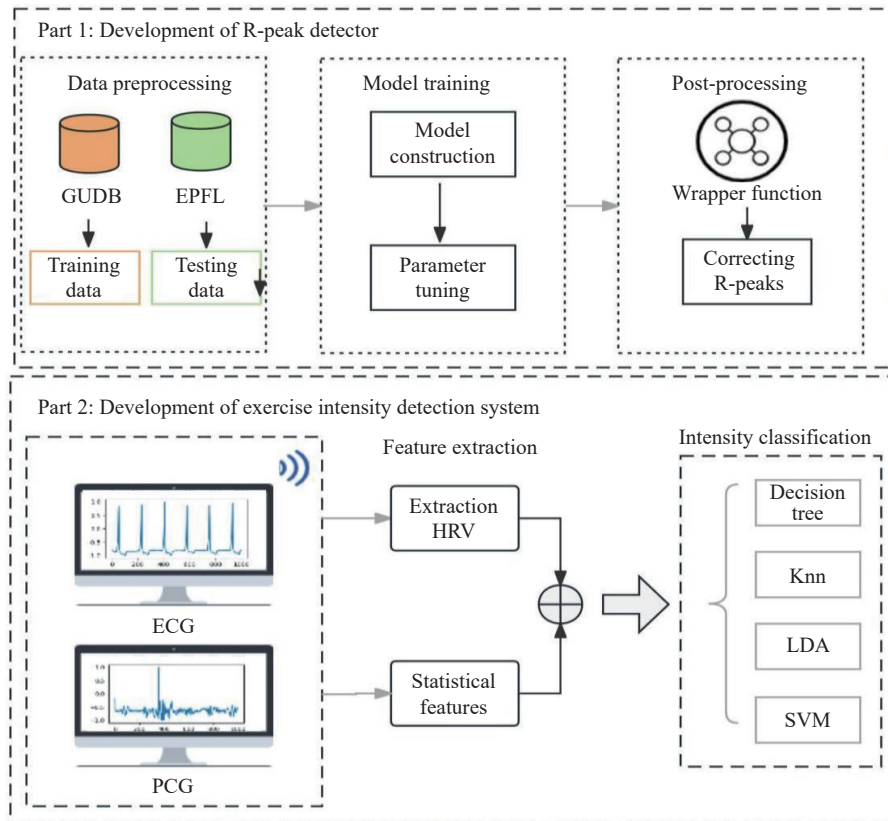


Fig. 1 Overall process of exercise intensity detection system

where  $x$  is the original input,  $z$  is the abstract feature representation of the input and  $\hat{y}$  is the spatial domain of the input.

**3.1.2 Training Data Preparation**

The data is divided into windows of 2 000 steps and is normalized to range  $[-1,1]$ . The binary marking strategy is used to mark each time step of the window. The position corresponding to the R peak is marked as “1”, and the others are marked as “0”. In order to slightly balance the label, two “1” markers were also added before and after the R peak position. This marking scheme can reduce the number of false positives [19].

**3.1.3 Model Architecture**

In the current, the Unet has been widely used for the R-peak detection. The main reason is that Unet has excellent feature extraction capabilities, which consists of 4 encoder blocks and 4 decoder blocks. The encoder down-samples the input through 4 layers of convolution, and the down-sampling factor is 2. For each layer, the convolution kernel sizes are set to 9, 6, 3 and 3, respectively. Each convolution is followed by batch normalization and rectified linear unit (RELU). In the decoder block, the compressed feature vec-

tor is up-sampled by the same number of transposed convolutions configured opposite to the encoder block. Fig. 2 and Fig. 3 shows our improvement on Unet by adding TCN. While Fig. 2 explains the concept of dilation rate for the Dilated Conv-1D in the TCN, which allows the convolution kernel to skip some elements in the input sequence, effectively expanding the receptive field and capturing wider context information.

**3.1.4 Training**

In our study, model optimization involves the utilization of binary cross-entropy loss and the Adam optimizer. To prevent over-fitting, we adopt the Model Checkpoint mechanism and the Early Stopping mechanism to save the best result.

**3.1.5 Wrapper Function**

In order to make the end-to-end R peak detection, we developed a set of wrapper functions, as shown in Fig. 4. Next, we will provide detailed explanations of steps 2 and 5.

Data Split: Overlapping window segments with a width of 1000 time steps are created, moving with user-defined strides (stride = 250, equivalent to four predictions per time step).

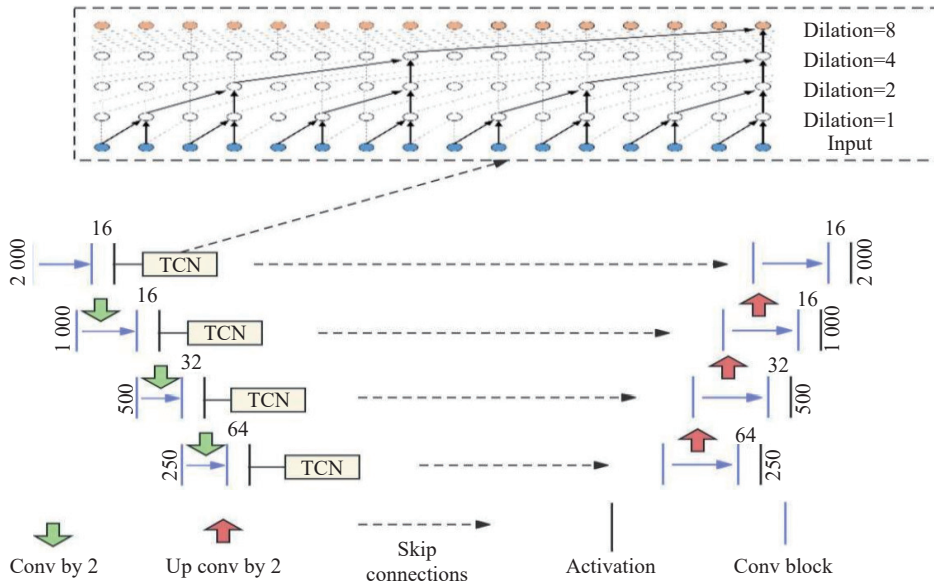


Fig. 2 Structure of Unet-TCN (the dilations means that for each convolutional layer, the sliding interval of the convolution kernel on the input is different. The choice of expansion factor affects the size of the receptive field of the convolutional layer and the ability of the model)

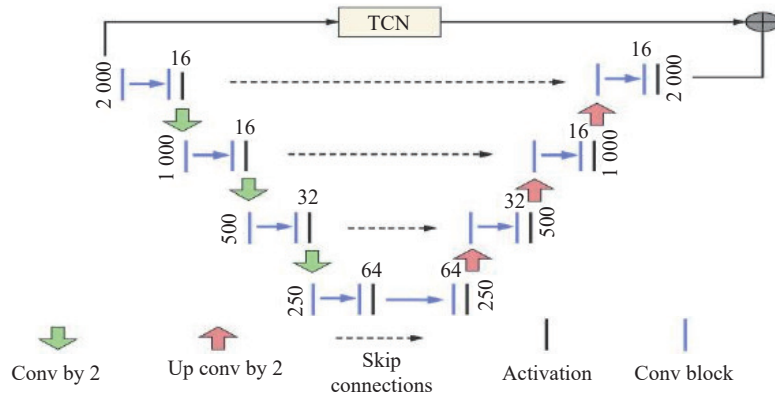


Fig. 3 Structure of Unet+TCN

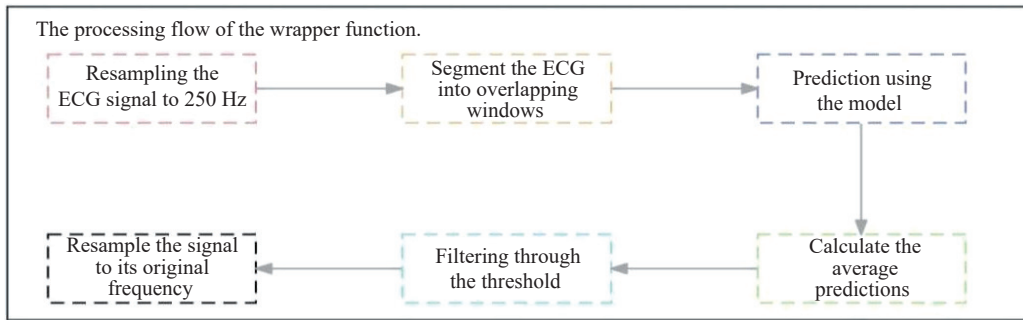


Fig. 4 The process of the wrapper function

While this increases computational cost, it enhances the accuracy of R-peak detection by capturing time step changes in different contexts.

**Filter Predictions:** After averaging overlapping predictions, each time step contains a probability value. Subsequently, the time steps are filtered based on a user-defined probability threshold. If five or more time steps are corrected to the same position, they are identified as an R-peak.

### 3.1.6 Experimental Result

To assess the effectiveness of the proposed R-peaks detector under high-intensity exercise, it is tested on the EPFL database. Training and testing with different datasets enables a more comprehensive evaluation of the detector's performance and ensures its robustness across unfamiliar data. To evaluate effectiveness, various evaluation metrics including Precision, Recall, and F1 score were calculated based on four main parameters: true positives (TP), true negatives (TN), false negatives (FN), and false positives (FP). These evaluation metrics are as follows:

$$\text{precision} = \frac{TP}{TP + FP} \quad (2)$$

$$\text{recall} = \frac{TP}{TP + FN} \quad (3)$$

$$\text{F1 score} = \frac{2 \times TP}{2 \times TP + FP + FN} \quad (4)$$

Predicted R-peak is considered true positive if it falls within one tenth of the sampling rate (25 samples at 250 Hz sampling rate) from the ground truth.

The experimental parameters utilized in this study, we select 0.1 as a user defined probability threshold and stride value of 250. From Tab. 1, it is clear that the proposed UNET-based method outperforms the classical methods with the entire test dataset. Under low-intensity exercise conditions (Seg\_1, Seg\_2, Seg\_5), because low-intensity exercise does not interfere with R-peak detection, the UNET-based method achieves F1 scores exceeding 0.997. The classical algorithms also achieve F1 scores exceeding 0.982, which indicates that the algorithm also shows significant improvement even under low intensity.

However, under high-intensity exercise conditions (Seg\_3, Seg\_4), the performance of traditional algorithms sharply decline, with some algorithms dropping below 0.90. This decline can be attributed to significant physiological changes during high-intensity exercise, such as increased heart rate, leading to notable alterations in ECG signal morphology that challenge traditional algorithms in R-peak detection. In contrast, deep learning algorithms (Unet and Unet-TCN) maintain strong performance. Unet-TCN outperforms Unet, thanks to TCN's enhanced ability to handle temporal relationships. However, the decline in performance for Unet + TCN may be due to information overlap from the direct connection between TCN and Unet, making it challenging to accurately distinguish each feature's contribution during processing.

Shaffer proposed that there is a problem with the default error tolerance (the default tolerance is a tenth of the sampling rate). At a sampling frequency of 250 Hz, this leads to a permissible error of 40 ms. Considering an average heart rate variability of 50 ms, any HRV becomes useless. Therefore, in this paper, one-fiftieth of the error tolerance rate is used to test the performance of our algorithm. Tab. 2 shows that Unet-TCN still maintains the best performance and has only a slight decrease compared

with the performance in Tab. 1. This further verifies the possibility of the algorithm in practical application.

### 3.1.7 Computation Time

All experiments are conducted on a system equipped with a 2.40 GHz Core i5-9300H processor and 16 GB of RAM. The testing is executed using a single CPU without employing a parallelized (CUDA) version. It takes about 378 ms for the Pan-Tompkins algorithm to detect 120 s ECG segments. In comparison, the time for Unet-TCN to detect the same ECG segments is about 904 ms, which indicates that the real-time speed is about 130 times. This may be slower when using Holter devices with low-configuration processors, but it is still much faster than real-time processing and can be used in embedded devices.

## 3.2 Exercise Intensity Detection

### 3.2.1 Data Processing

The EPHNOGRAM dataset [19] is used to evaluate the performance of the exercise intensity detection system. This dataset comprises six modes, including lying in bed, sitting, walking at a constant speed, pedaling a stationary bike, bike load test, and Bruce treadmill load test. These modes were categorized into six exercise intensities, labeled from 1 to 6. The data were down-sampled to 250 Hz and normalized to range

Tab. 1 The performance of different R-peak detectors (tolerance rate of 1/10)

Intensity		Unet-TCN	Unet	Unet + TCN	Christov	Engzee	Hamilton	Pan-Tompkins
Seg_1	Preci	0.997	0.994	0.998	<b>1.0</b>	0.994	0.918	0.997
	recall	<b>0.999</b>	0.998	0.998	0.973	0.98	0.916	0.984
	F1	<b>0.998</b>	0.996	<b>0.998</b>	0.984	0.991	0.917	0.991
Seg_2	Preci	0.991	0.990	<b>0.998</b>	0.998	0.987	0.893	0.998
	recall	<b>0.998</b>	0.997	0.998	0.968	0.975	0.889	0.982
	F1	<b>0.994</b>	0.993	<b>0.998</b>	0.980	0.981	0.891	0.990
Seg_3	Preci	<b>0.991</b>	0.980	0.989	0.982	0.940	0.718	0.997
	recall	<b>0.995</b>	0.990	0.932	0.904	0.901	0.708	0.819
	F1	<b>0.993</b>	0.985	0.953	0.935	0.917	0.713	0.883
Seg_4	Preci	<b>0.991</b>	0.977	0.989	0.979	0.900	0.716	0.992
	recall	<b>0.997</b>	0.990	0.921	0.875	0.851	0.707	0.850
	F1	<b>0.994</b>	0.983	0.945	0.904	0.872	0.711	0.906
Seg_5	Preci	<b>0.999</b>	0.997	0.999	0.999	0.981	0.998	0.999
	recall	<b>0.997</b>	0.997	0.996	0.976	0.964	0.987	0.983
	F1	<b>0.998</b>	0.997	0.997	0.985	0.972	0.992	0.991

Tab. 2 The performance of different R-peak detectors (tolerance rate of 1 / 50)

Intensity		Unet-TCN	Unet	Unet + TCN	Christov	Engzee	Hamilton	Pan-Tompkins
Seg_1	Preci	<b>1.0</b>	0.995	0.999	1.0	0.994	0.999	1.0
	recall	<b>0.999</b>	0.999	0.999	0.973	0.98	0.997	0.986
	F1	<b>0.999</b>	0.997	0.999	0.984	0.991	0.998	0.993
Seg_2	Preci	0.997	0.990	0.998	<b>1.0</b>	0.989	0.996	<b>1.0</b>
	recall	<b>0.998</b>	0.997	0.998	0.969	0.977	0.991	0.983
	F1	<b>0.998</b>	0.993	0.998	0.982	0.983	0.993	0.991
Seg_3	Preci	<b>0.994</b>	0.984	0.991	0.989	0.942	0.980	0.995
	recall	<b>0.990</b>	0.994	0.935	0.908	0.902	0.964	0.824
	F1	<b>0.992</b>	0.989	0.955	0.940	0.919	0.972	0.889
Seg_4	Preci	<b>0.995</b>	0.980	0.994	0.983	0.908	0.978	0.996
	recall	0.992	<b>0.993</b>	0.924	0.878	0.856	0.963	0.852
	F1	<b>0.993</b>	0.986	0.949	0.909	0.878	0.970	0.909
Seg_5	Preci	<b>0.999</b>	0.997	0.999	0.999	0.981	0.998	0.999
	recall	<b>0.997</b>	0.997	0.996	0.976	0.964	0.987	0.983
	F1	<b>0.998</b>	0.997	0.997	0.985	0.972	0.992	0.991

$[-1,1]$ . After splitting the data, each sample consists of 2 000 time step (approximately 8–10 complete ECG cycles).

### 3.2.2 Feature Extraction

To achieve faster and real-time exercise intensity detection, the classification is mainly based on the HRV and linear features of PCG. This is also an exploration of multi-modal feature fusion. HRV refers to the interval change between heart beats, which is usually used to reflect the regulation of autonomic nervous system on cardiac activity. The linear features of PCG can be used to describe various properties of the heart sound signal, such as its morphology, spectrum, and dynamic range. The details are shown in Tab. 3.

### 3.2.3 Experimental Results

To ensure an objective and fair evaluation of the system, a five-fold cross-validation strategy is adopted. To evaluate effectiveness, various evaluation metrics including Sensitivity, Specificity, and Accuracy were calculated based on four main parameters: true positives (TP), true negatives (TN), false negatives (FN), and false positives (FP).

$$Se = \frac{TP}{TP + FN} \quad (5)$$

$$Sp = \frac{TN}{TN + FP} \quad (6)$$

$$Acc = \frac{TP + TN}{TP + TN + FP + FN} \quad (7)$$

Sensitivity represents the proportion of actual positive cases, specificity represents the proportion of actual negative cases and accuracy represents the overall correctness of the model’s predictions across all classes. Additionally, we compare the performance of different classifiers, various R-peak detectors, and the impact of feature fusion on exercise intensity detection accuracy. The following section will provide a detailed overview of the related experiments.

Initially, the proposed R-peak detector (Unet-TCN) is integrated into the exercise intensity detection system to identify R-peak positions for HRV extraction. Subsequently, classification is performed using different classifiers, and their performances as shown in Tab. 4. The results indicate that decision trees exhibits superior effectiveness, attributed to their adaptability to diverse data types and their capability to capture non-linear relationships.

Secondly, different R-peak detectors are integrated into the exercise intensity detection system. As shown in Tab. 5, accurate R-peak detection directly impacts the accuracy of exercise intensity detection. The performance of traditional R-peak detectors is nearly identical. Com-

**Tab. 3 Features used for exercise intensity detection**

Signal type	Feature type	Feature description
ECG	Time domain feature	SDSD: Standard deviation of difference between R-R intervals.
		SDNN: Standard deviation of NN (R-R) intervals.
		RMSSD: Root mean square of the Autonomic nervous system's parasympathetic branch.
		Mean ( HRV-NNX ): Mean value of RR intervals.
		PNN50: Proportion of NN50 divided by total NN (R-R) intervals.
	Frequency domain feature	Mean (PLF) : Average percentage of low frequency components.
		Mean (PHF): Average percentage of high frequency components.
		Mean (LFHF ratio) : Average LF/HF ratio.
		Mean (SD1): Average short axis (SD1) in the Poincaré plot.
		Mean (SD2): Average long axis (SD2) in the Poincaré plot.
PCG	Linear feature	Mean (SD1 SD2 ratio) : Average of SD1 and SD2 ratios.
		Mean_pcg: Mean value of PCG signal.
		Std_deviation_pcg: Standard deviation of PCG signal.
		Variance_pcg: Variance of PCG signal.
		Max_pcg: Maximum value of PCG signal.
		Min_pcg: Minimum value of PCG signal.
		Skewness_pcg: Skewness of PCG signal distribution.

**Tab. 4 The classification results using different ML classifiers**

Performance	Unet-Tcn	Hamilton	Christov	Engzee	Pan-Tompkins
Se (%) ( recall )	0.967	0.941	0.937	0.939	0.942
Sp (%)	0.902	0.825	0.811	0.817	0.826
Acc (%)	0.981	0.965	0.962	0.963	0.965

pared to traditional R-peak detectors, the proposed R-peak detector improves the accuracy of exercise intensity detection by 1.6% and recall by 2.7%.

**Tab. 5 The classification results using different R-peak detector**

Performance	Decision tree	Knn	LDA	SVM(RBF)
Se (%) ( recall )	0.933	0.877	0.859	0.825
Sp (%)	0.801	0.632	0.563	0.477
Acc (%)	0.981	0.940	0.901	0.890

Finally, single-signal features and multi-signal features are respectively utilized to compare the impact of multiple signal modes on exercise intensity detection. As shown in [Tab. 6](#), the multi-modal feature fusion contributes to enhancing the accuracy of exercise intensity detection.

**Tab. 6 The impact of feature fusion on sports fatigue detection**

Features	Se (%)	Sp (%)	Acc (%)
Only HRV features	0.933	0.802	0.960
Only PCG features	0.866	0.601	0.920
PCG features and HRV features	0.967	0.902	0.981

## 4 Conclusion

A method for exercise intensity detection utilizing HRV is proposed in this study. To accurately extract HRV, we developed an R-peak detector to detect R-peaks under high-intensity exercise conditions. The detector was developed based on the Unet and TCN models. The detector was tested on real datasets and met the requirements for practical applications in terms of both detection accuracy and speed. Additionally, to further enhance the precision of exercise intensity detection, we explored multi-modal feature fusion. The fusion of features from ECG and PCG signals significantly improved the accuracy of detection. In future research, we will continue to explore information within ECG and PCG signals, aiming to fully leverage the available information.

## References:

- [1] A. Kathryn, E. Justus, and R. Angela, "The effects of training status and exercise intensity on exer-

- cise-induced muscle damage, ” *The Journal of Sports Medicine and Physical Fitness*, vol. 60, no. 3, pp. 449-455, 2020.
- [2] T. Beukelaar and D. Mantini, “Monitoring resistance training in real time with wearable technology: Current applications and future directions, ” *Bioengineering*, vol. 10, no. 9, pp. 1085, 2023.
- [3] S. Chen, H. Zhao, and X. Chen, “Detecting sports fatigue from speech by support vector machine, ” in *IEEE International Conference on Communication Software and Networks (ICCSN)*, IEEE, 2016.
- [4] J. Wilson and M. Jacob, “Non-traditional immersive seminar enhances learning by promoting greater physiological and psychological engagement compared to a traditional lecture format, ” *Physiology & Behavior*, vol. 238, pp. 113461, 2021.
- [5] S. Kaufmann and H. Herold, “Heart rate variability-derived thresholds for exercise intensity prescription in endurance sports: A systematic review of interrelations and agreement with different ventilatory and blood lactate thresholds, ” *Sports Medicine-Open*, vol. 9, pp. 59, 2023.
- [6] W. Yu and X. Han, “Wearable heart rate monitoring intelligent sports bracelet based on internet of things, ” *Measurement*, vol. 164, pp. 108102, 2020.
- [7] G. Parfitt and S. Hughes, “The exercise intensity-affect relationship: Evidence and implications for exercise behavior, ” *Journal of Exercise Science & Fitness*, vol. 7, no. 2, pp. 34-41, 2020.
- [8] H. S. Zeng and Y. Zhao. “Sensing movement: Microsensors for body motion measurement, ” *Sensors*, vol. 11, no. 1, pp. 638-660, 2011.
- [9] D. Bok, M. Rakovac, and C. Foster, “An examination and critique of subjective methods to determine exercise intensity: the talk test, feeling scale, and rating of perceived exertion, ” *Sports Medicine*, vol. 52, no. 9, pp. 2085-2109, 2022.
- [10] R. Pero, M. Brancaccio, and C. Mennitti, “Urinary biomarkers: Diagnostic tools for monitoring athletes’ health status, ” *International Journal of Environmental Research and Public Health*, vol. 17, pp. 6065, 2020.
- [11] J. Dong and W. Ji, “Recognition of adolescent exercise intensity based on LSTM network and ECG signal, ” *Printing and Digital Media Technology Research*, vol. 6, pp. 49-58, 2023.
- [12] Y. Chen, X. Ma, X. Su, and H. Ge, “Classification of exercise fatigue by fusing image features and linear features of ECG, ” in *Proceedings of the 13th National Sports Science Conference*, abstract collection of special reports, Sports Engineering Branch, 2023.
- [13] S. Sarmiento, “Heart rate variability during high-intensity exercise, ” *Journal of Systems Science and Complexity*, vol. 26, pp. 104-116, 2013.
- [14] J. P. Pan and W. J. Tompkins, “A real-time QRS detection algorithm, ” *IEEE Transactions on Biomedical Engineering*, vol. 3, pp. 230-236, 1985.
- [15] J. Laitala, “Robust ECG R-peak detection using LSTM, ” in *Proceedings of the 35th Annual ACM Symposium on Applied Computing*, 2020.
- [16] M. U. Zahid, “Robust R-peak detection in low-quality holter ECGs using 1D convolutional neural network, ” *IEEE Transactions on Biomedical Engineering*, vol. 69, no. 1, pp. 119-128, 2021.
- [17] B. Porr and L. Howell, “R-peak detector stress test with a new noisy ECG database reveals significant performance differences amongst popular detectors, ” *BioRxiv*, vol. 10, pp. 722397, 2019.
- [18] A. Kazemnejad, P. Gordany, and R. Sameni, “An open-access simultaneous electrocardiogram and phonocardiogram database, ” *BioRxiv*, vol. 45, no. 5, pp. 055005, 2021.
- [19] F. Shaffer and P. Ginsberg, “An overview of heart rate variability metrics and norms, ” *Frontiers in Public Health*, vol. 5, pp. 258, 2017.



sis.

**Xinhua Su** received the Ph.D. degree from Beijing Institute of Technology, China, in 2020. She is currently a Lecturer with School of Sports Engineering, Beijing Sport University, Beijing, China. Her research interests include image and signal processing, and sports data analysis.



**Xuxuan Wang** is currently a master student with School of Sports Engineering, Beijing Sport University. His research interests are changes in physiological signals during exercise.



**Xinxin Ma** is currently a master student with School of Sports Engineering, Beijing Sport University. Her research interests are changes in physiological signals during exercise.